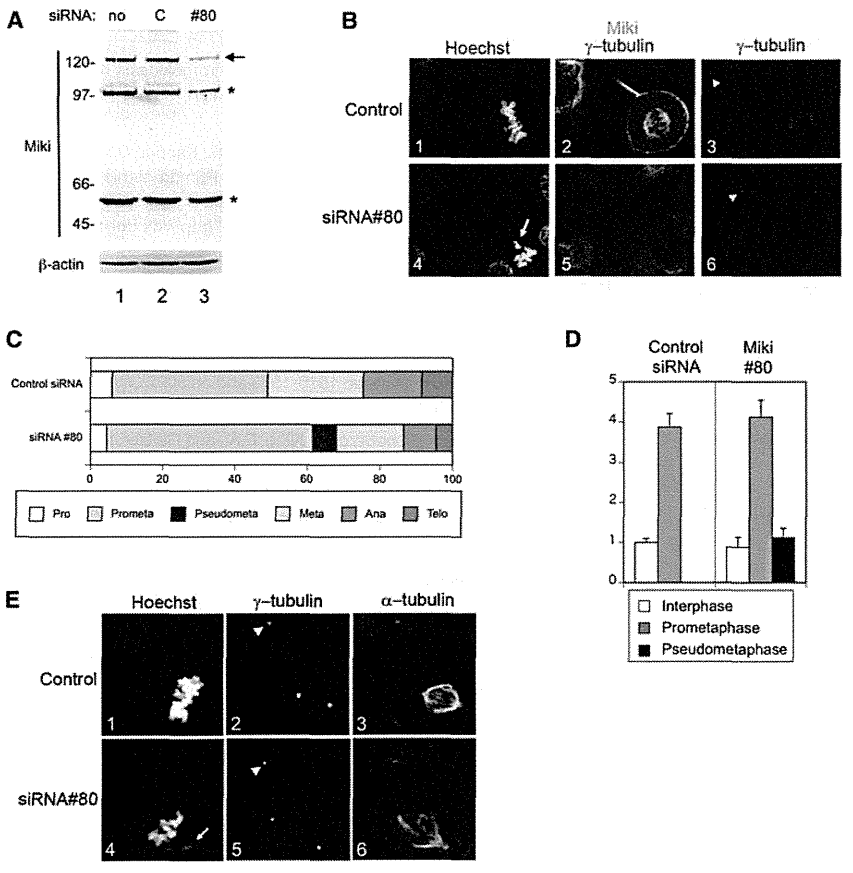


**Figure 6. Mitotic Disturbance by Miki Downregulation in hRPE Cells**

(A) Miki and β-actin immunoblots of hRPE cells (lane 1), cells treated with control siRNA (lane 2), or siRNA#80 (lane 3) (100 nM for 48 hr). Arrows indicate position of p125; asterisks, unidentified bands.

(B and E) Immunostaining of cells treated with the siRNA indicated on the left using the antibodies indicated above. DNA was stained with Hoechst 33342.

(C) Cells were treated with the siRNA indicated at the left for 48 hr. Percentages of the 500 cells in each mitotic phase or undergoing abnormal mitosis were calculated from observations of Hoechst 33342-stained nuclei. Asterisks indicate significant changes relative to the control.

(D) Relative fluorescence intensity of γ-tubulin in centrosomes at interphase (open bars), prometaphase (gray bar), or pseudometaphase (black bar) in cells treated with the siRNAs indicated above. Shown is average with SD (20 centrosomes).

for 48 hr were detached from the coverslip by gentle pipetting. Detached cells were then added to another coverslip, on which cells had been cultured with control siRNA for 48 hr. After culture for an additional 3 hr, the coverslip containing mitotic cells treated with both specific or control siRNA was immunostained according to methods previously described (Oshimori et al., 2006; Tokai-Nishizumi et al., 2005). Relative fluorescence intensity was measured using ImageJ software.

### Tankyrase-1 PARP Assay

A cDNA encoding hexameric His-tagged human Mikiα was cloned into pTD1 (Shimadzu, Kyoto, Japan) and mRNA synthesized in vitro using the Megascript system (Ambion, Foster City, CA). Protein synthesized in vitro using the Transdirect insect cell system (Shimadzu) was purified on Ni-NTA beads. Tankyrase-1 was immunoprecipitated from HeLa cells that had been synchronized at G1 or G2/M phase using the standard double-thymidine method. PARP assays were performed using 1 μg purified Miki, tankyrase-1 bound to protein G beads, and [$^{32}$P]NAD$^+$ according to the method previously described (Seimiya et al., 2004).

### Mitosis Analysis

Floating mitotic cells were counted by detaching cells by gentle pipetting and staining with trypan blue to exclude apoptotic cells. Chromosome velocities were measured in U2OS cells expressing an H2B-GFP fusion protein using methods described previously (Levesque and Compton, 2001). Nocodazole sensitivity and cold tests were performed as described previously (Oshimori et al., 2006; Tokai-Nishizumi et al., 2005). The ratio of tubulin polymers to dimers was quantified based on a procedure described previously (Mishima et al., 2004). Mitotic spindles were isolated according to a previously described method (Sillje and Nigg, 2006). Briefly, synchronized HeLa cells at the G2/M boundary were detached from the plate by gentle tapping and then incubated for an additional 30 min. Cells mostly (>90%) in metaphase or early anaphase were lysed with hypotonic buffer containing taxol and ADP-HDP (30 μM; Merck), a PARG inhibitor. Then, by removing soluble cytosolic and membrane/actin-associated proteins as well as intermediate filaments by centrifugation, mitotic spindles/centrosomes were isolated. Microtubule regrowth assays were performed by completely depolymerizing tubules in cells with 10 mM nocodazole on ice for 60 min. Cells were washed three times with serum-free medium and then incubated in warm medium at 37°C.

### Other Experimental Procedures and Reagents

Immunoprecipitation and immunoblotting were performed according to standard procedures (Shinjyo et al., 2001) using 2% gelatin as a blocking agent. Mass spectrometry was performed by methods described in the Supplemental Experimental Procedures. Antibodies to pericentrin/kendrin,

**Figure 5. Miki Induces γ-TuRC Formation in Mitotic Centrosomes**

(A–C and G) Immunostaining of HeLa cells treated with siRNA indicated above for 48 hr with anti-γ-tubulin antibody. DNA was stained using Hoechst 33342 (left). Arrows or arrowheads indicate centrosomes at interphase or prometaphase, respectively (A and C). Relative fluorescence intensity of proteins indicated below in centrosomes at interphase (open bars), prometaphase (gray bars), or pseudometaphase (black bars) (right panel). To evaluate intensity, centrosomal areas were enriched by the edge of γ-tubulin staining, and the mean intensity in each was measured and the background levels subtracted. Shown is average with SD (100 centrosomes).

(D) HeLa cells (Pt) were treated with the siRNA (100 nM) indicated above for 48 hr. Shown is immunoblot analysis using antibodies indicated at left.

(E and F) HeLa cells were treated with the siRNA (100 nM) indicated above for 48 hr. Shown is immunostaining of cells at metaphase or pseudometaphase using antibodies indicated. Arrows indicate the position of mitotic centrosomes (E).

CG-NAP, and GCP2 were kind gifts of Drs. M. Takahashi and Y. Ono (Takahashi et al., 2002). Rabbit anti-Miki polyclonal antibody was described elsewhere (Asou et al., 2009). Commercial antibodies were obtained from the following suppliers: actin (1378 996) from Roche; α-tubulin (T9026) and γ-tubulin (T6557) from Sigma, tankyrase-1 (H-350) from Santa Cruz Biotechnologies, PAR (10H) from Trevigen, and p230 (#15) from BD Bioscience, ch-TOG (QED). 3-aminobenzamide was purchased from Merck; Hoechst 33342 from Invitrogen; and thymidine, aphidicolin, and nocodazole from Sigma.

## SUPPLEMENTAL INFORMATION

Supplemental Information includes four figures, four movies, and Supplemental Experimental Procedures and can be found with this article at http://dx.doi.org/10.1016/j.molcel.2012.06.033.

## ACKNOWLEDGMENTS

We thank Drs. N. Oshimori and N. Tokai-Nishizumi for establishment of cell lines and helpful discussion and Ms. M. Nakamura and Mr. N. Yamazaki for excellent technical assistance. This work was supported by Grants-in-Aid for Scientific Research from the Ministry of Education, Culture, Sports, Science, and Technology of Japan.

Received: November 28, 2011
Revised: February 28, 2012
Accepted: June 19, 2012
Published online: August 2, 2012

## REFERENCES

Asou, H., Matsui, H., Ozaki, Y., Nagamachi, A., Nakamura, M., Aki, D., and Inaba, T. (2009). Identification of a common microdeletion cluster in 7q21.3 subband among patients with myeloid leukemia and myelodysplastic syndrome. Biochem. Biophys. Res. Commun. *383*, 245–251.

Blagden, S.P., and Glover, D.M. (2003). Polar expeditions—provisioning the centrosome for mitosis. Nat. Cell Biol. *5*, 505–511.

Brouhard, G.J., Stear, J.H., Noetzel, T.L., Al-Bassam, J., Kinoshita, K., Harrison, S.C., Howard, J., and Hyman, A.A. (2008). XMAP215 is a processive microtubule polymerase. Cell *132*, 79–88.

Chang, P., Jacobson, M.K., and Mitchison, T.J. (2004). Poly(ADP-ribose) is required for spindle assembly and structure. Nature *432*, 645–649.

Chang, P., Coughlin, M., and Mitchison, T.J. (2005a). Tankyrase-1 polymerization of poly(ADP-ribose) is required for spindle structure and function. Nat. Cell Biol. *7*, 1133–1139.

Chang, W., Dynek, J.N., and Smith, S. (2005b). NuMA is a major acceptor of poly(ADP-ribosyl)ation by tankyrase 1 in mitosis. Biochem. J. *391*, 177–184.

Chi, N.W., and Lodish, H.F. (2000). Tankyrase is a golgi-associated mitogen-activated protein kinase substrate that interacts with IRAP in GLUT4 vesicles. J. Biol. Chem. *275*, 38437–38444.

Dynek, J.N., and Smith, S. (2004). Resolution of sister telomere association is required for progression through mitosis. Science *304*, 97–100.

Gergely, F., Draviam, V.M., and Raff, J.W. (2003). The ch-TOG/XMAP215 protein is essential for spindle pole organization in human somatic cells. Genes Dev. *17*, 336–341.

Gordon, M.B., Howard, L., and Compton, D.A. (2001). Chromosome movement in mitosis requires microtubule anchorage at spindle poles. J. Cell Biol. *152*, 425–434.

Keryer, G., Di Fiore, B., Celati, C., Lechtreck, K.F., Mogensen, M., Delouvee, A., Lavia, P., Bornens, M., and Tassin, A.M. (2003). Part of Ran is associated with AKAP450 at the centrosome: involvement in microtubule-organizing activity. Mol. Biol. Cell *14*, 4260–4271.

Kuribara, R., Kinoshita, T., Miyajima, A., Shinjyo, T., Yoshihara, T., Inukai, T., Ozawa, K., Look, A.T., and Inaba, T. (1999). Two distinct interleukin-3-mediated signal pathways, Ras-NFIL3 (E4BP4) and Bcl-xL, regulate the survival of murine pro-B lymphocytes. Mol. Cell. Biol. *19*, 2754–2762.

Levesque, A.A., and Compton, D.A. (2001). The chromokinesin Kid is necessary for chromosome arm orientation and oscillation, but not congression, on mitotic spindles. J. Cell Biol. *154*, 1135–1146.

Li, C.F., MacDonald, J.R., Wei, R.Y., Ray, J., Lau, K., Kandel, C., Koffman, R., Bell, S., Scherer, S.W., and Alman, B.A. (2007). Human sterile alpha motif domain 9, a novel gene identified as down-regulated in aggressive fibromatosis, is absent in the mouse. BMC Genomics *8*, 92. http://dx.doi.org/10.1186/1471-2164-8-92.

Mauritzson, N., Albin, M., Rylander, L., Billstrom, R., Ahlgren, T., Mikoczy, Z., Bjork, J., Stromberg, U., Nilsson, P.G., Mitelman, F., et al. (2002). Pooled analysis of clinical and cytogenetic features in treatment-related and de novo adult acute myeloid leukemia and myelodysplastic syndromes based on a consecutive series of 761 patients analyzed 1976-1993 and on 5098 unselected cases reported in the literature 1974-2001. Leukemia *16*, 2366–2378.

Mishima, M., Pavicic, V., Gruneberg, U., Nigg, E.A., and Glotzer, M. (2004). Cell cycle regulation of central spindle assembly. Nature *430*, 908–913.

Nigg, E.A. (2002). Centrosome aberrations: cause or consequence of cancer progression? Nat. Rev. Cancer *2*, 815–825.

Oshimori, N., Ohsugi, M., and Yamamoto, T. (2006). The Plk1 target Kizuna stabilizes mitotic centrosomes to ensure spindle bipolarity. Nat. Cell Biol. *8*, 1095–1101.

Oshimori, N., Li, X., Ohsugi, M., and Yamamoto, T. (2009). Cep72 regulates the localization of key centrosomal proteins and proper bipolar spindle formation. EMBO J. *28*, 2066–2076.

Ozaki, Y., Matsui, H., Nagamachi, A., Asou, H., Aki, D., and Inaba, T. (2011). The dynactin complex maintains the integrity of metaphasic centrosomes to ensure transition to anaphase. J. Biol. Chem. *286*, 5589–5598.

Seimiya, H., Muramatsu, Y., Smith, S., and Tsuruo, T. (2004). Functional subdomain in the ankyrin domain of tankyrase 1 required for poly(ADP-ribosyl)ation of TRF1 and telomere elongation. Mol. Cell. Biol. *24*, 1944–1955.

Shi, Q., and King, R.W. (2005). Chromosome nondisjunction yields tetraploid rather than aneuploid cells in human cell lines. Nature *437*, 1038–1042.

Shinjyo, T., Kuribara, R., Inukai, T., Hosoi, H., Kinoshita, T., Miyajima, A., Houghton, P.J., Look, A.T., Ozawa, K., and Inaba, T. (2001). Downregulation of Bim, a proapoptotic relative of Bcl-2, is a pivotal step in cytokine-initiated survival signaling in murine hematopoietic progenitors. Mol. Cell. Biol. *21*, 854–864.

Sillje, H.H., and Nigg, E.A. (2006). Purification of mitotic spindles from cultured human cells. Methods *38*, 25–28.

Takahashi, M., Yamagiwa, A., Nishimura, T., Mukai, H., and Ono, Y. (2002). Centrosomal proteins CG-NAP and kendrin provide microtubule nucleation sites by anchoring gamma-tubulin ring complex. Mol. Biol. Cell *13*, 3235–3245.

Tokai-Nishizumi, N., Ohsugi, M., Suzuki, E., and Yamamoto, T. (2005). The chromokinesin Kid is required for maintenance of proper metaphase spindle size. Mol. Biol. Cell *16*, 5455–5463.

Vaughan, K.T. (2005). TIP maker and TIP marker; EB1 as a master controller of microtubule plus ends. J. Cell Biol. *171*, 197–200.

Weaver, B.A., Bonday, Z.Q., Putkey, F.R., Kops, G.J., Silk, A.D., and Cleveland, D.W. (2003). Centromere-associated protein-E is essential for the mammalian mitotic checkpoint to prevent aneuploidy due to single chromosome loss. J. Cell Biol. *162*, 551–563.

Yeh, T.Y., Sbodio, J.I., and Chi, N.W. (2006). Mitotic phosphorylation of tankyrase, a PARP that promotes spindle assembly, by GSK3. Biochem. Biophys. Res. Commun. *350*, 574–579.

Zimmerman, W.C., Sillibourne, J., Rosa, J., and Doxsey, S.J. (2004). Mitosis-specific anchoring of gamma tubulin complexes by pericentrin controls spindle organization and mitotic entry. Mol. Biol. Cell *15*, 3642–3657.

bjh research paper

# Identification of the integrin β3 L718P mutation in a pedigree with autosomal dominant thrombocytopenia with anisocytosis

**Yoshiyuki Kobayashi,[1,2] Hirotaka Matsui,[1]* Akinori Kanai,[1] Miyuki Tsumura,[2] Satoshi Okada,[2] Mizuka Miki,[2] Kazuhiro Nakamura,[2] Shinji Kunishima,[3] Toshiya Inaba[1] and Masao Kobayashi[2]**

*[1]Department of Molecular Oncology and Leukaemia Programme Project, Research Institute for Radiation Biology and Medicine, Hiroshima University, [2]Department of Paediatrics, Graduate School of Biomedical and Health Sciences, Hiroshima University, Minami-ku, Hiroshima, and [3]Department of Advanced Diagnosis, Clinical Research Centre, National Hospital Organization Nagoya Medical Centre, Nagoya, Aichi, Japan*

Received 29 June 2012; accepted for publication 22 October 2012

Correspondence: Hirotaka Matsui, Department of Molecular Oncology and Leukemia Program Project, Research Institute for Radiation Biology and Medicine, Hiroshima University, 1-2-3 Kasumi, Minami-ku, Hiroshima 734-8553, Japan.
E-mail: hmatsui@hiroshima-u.ac.jp

## Summary

αIIbβ3 integrin mutations that result in the complete loss of expression of this molecule on the platelet surface cause Glanzmann thrombasthenia. This is usually autosomal recessive, while other mutations are known to cause dominantly inherited macrothrombocytopenia (although such cases are rare). Here, we report a 4-generation pedigree including 10 individuals affected by dominantly inherited thrombocytopenia with anisocytosis. Six individuals, whose detailed clinical and laboratory data were available, carried a non-synonymous *ITGB3* gene alteration resulting in mutated integrin β3 (ITGB3)-L718P. This mutation causes partial activation of the αIIbβ3 complex, which promotes the generation of abnormal pro-platelet-like protrusions through downregulating RhoA (RHOA) activity in transfected Chinese Hamster Ovary cells. These findings suggest a model whereby the integrin β3-L718P mutation contributes to thrombocytopenia through gain-of-function mechanisms.

**Keywords:** integrin β3 L718P mutation, familial thrombocytopenia, autosomal dominant inheritance, whole exome sequencing, inhibition of RhoA.

Lifelong haemorrhagic syndromes are in part caused by point mutations in the *ITGA2B* and *ITGB3* genes encoding ITGA2B and ITGB3 proteins (integrin αIIb and β3, respectively). The αIIbβ3 complex regulates thrombopoiesis by megakaryocytes and aggregation of platelets in response to extracellular stimuli, such as ADP and collagen. The autosomal recessive syndrome, Glanzmann thrombasthenia, is the most frequently encountered disease caused by αIIbβ3 mutations (George *et al*, 1990; Nurden, 2006; Nurden & Nurden, 2008; Nurden *et al*, 2011a). Patients have a homozygous or a compound heterozygous mutation in the *ITGA2B* or *ITGB3* genes that causes loss of function of the αIIbβ3 complex. Although platelet counts and size are generally normal, patients typically have severe mucocutaneous bleeding, such as epistaxis, menorrhagia and gastrointestinal bleeding, frequently because of defects in platelet aggregation.

Mutations of the αIIbβ3 complex are also involved in congenital haemorrhagic diseases other than Glanzmann thrombasthenia (Ghevaert *et al*, 2008; Schaffner-Reckinger *et al*, 2009; Jayo *et al*, 2010; Kunishima *et al*, 2011; Nurden *et al*, 2011b). For example, the integrin β3 D723H mutation is found in autosomal dominant macrothrombocytopenia (Ghevaert *et al*, 2008). Biochemical analysis revealed that integrin β3-D723H is a gain of function mutation which activates the αIIbβ3 complex constitutively, albeit only partially. This results in the formation of proplatelet-like protrusions in transfected Chinese Hamster Ovary (CHO) cells, a model of relevance for the formation of macrothrombocytes (Ghevaert *et al*, 2008; Schaffner-Reckinger *et al*, 2009).

More recently, a sporadic patient carrying an integrin β3-L718P mutation was reported (Jayo *et al*, 2010). She had mild thrombocytopenia ($127 \times 10^9$/l), platelet anisocytosis and reduced platelet aggregation potential. This mutation also induces abnormal proplatelet formation.

In the present study, we report a pedigree with a total 10 of individuals affected by a dominantly inherited haemorrhagic

© 2012 Blackwell Publishing Ltd

First published online 17 December 2012
doi:10.1111/bjh.12160

syndrome. Six individuals whose detailed clinical and laboratory data are available, presented with thrombocytopenia accompanied by anisocytosis and carry a non-synonymous *ITGB3* T2231C alteration resulting in the integrin β3-L718P mutation. We also performed entire exon sequencing by a next-generation sequencing and found that the integrin β3-L718P mutation is most likely the sole gene responsible for thrombocytopenia in this pedigree.

## Materials and methods

Written informed consent was obtained from individuals in the family in accordance with the Declaration of Helsinki for blood sampling and analysis undertaken with the approval of the Hiroshima University Institutional Review Board.

### *Patient*

The patient was 4-year-old Japanese girl (iv.3 in Fig 1A), who presented with mild bleeding tendencies, such as recurrent nasal bleeding and purpura in her extremities. Her platelet count was 49–72 × $10^9$/l with a mean platelet volume (MPV) of 9·8–10·9 fl. White blood cell and red blood cell counts were within the normal range and there were no morphological abnormalities including inclusions in neutrophils. Bone marrow examination was not performed. A total of six of her relatives, namely her father (iii.2), sister and brother (iv.1 and iv.2), two cousins (iv.4 and iv.5) and an aunt (iii.5), were subsequently found to have low platelet counts and were referred to our institute for further investigation.

### *Antibodies and reagents*

Unconjugated or phycoerythrin-cyanin 5 (PC5)-conjugated anti-CD41 monoclonal antibody (Ab) (clone P2) against the αIIbβ3 complex (Beckman Coulter, Brea, CA, USA), fluorescein isothiocyanate (FITC)-conjugated anti-CD41a monoclonal Ab (clone HIP8) (Beckman Coulter), FITC- or peridinin chlorophyll (PerCP)-conjugated anti-CD61 monoclonal Ab (clone RUU-PL 7F12) (BD Biosciences, San Jose, CA, USA), FITC-conjugated PAC-1 (BD Biosciences) and Alexa488-conjugated human fibrinogen (Life Technologies, Carlsbad, CA, USA) were used in flow cytometry. Anti-CD61 monoclonal Ab (clone EP2417Y) (Abcam, Cambridge, UK), anti-DDDDK-tag polyclonal Ab (Medical & Biological Laboratories, Nagoya, Japan), Alexa488-conjugated phalloidin and Hoechst 33342 (both Life Technologies) were used for immunofluorescence microscopy. The oligopeptide Arg-Gly-Asp-Ser (RGDS) (Sigma–Aldrich, St Louis, MO, USA) was used to competitively inhibit the binding of ligands to αIIbβ3, and adenosine diphosphate (ADP) (nacalai tesque, Kyoto, Japan) was used for the stimulation of αIIbβ3 on platelets.

### *Construction and transfection of expression vectors*

Full-length wild type (WT) *ITGA2B* and *ITGB3* cDNA were amplified by polymerase chain reaction (PCR) and cloned into pcDNA3·1 expression vectors. A PCR-mediated site-directed mutagenesis technique was applied to produce *ITGB3* mutants encoding integrin β3-L718P, -D723H and -T562N with or without truncation at the C-terminal side of $Y^{759}$ (del. 759). *RHOA* cDNA, which encodes RhoA (RHOA) protein, was amplified by PCR and its mutants (T19N and Q63L) were generated by site-directed mutagenesis, followed by cloning into p3xFLAG-CMV-10 vectors (Sigma–Aldrich). The *ITGA2B* and *ITGB3* expression vectors were simultaneously transfected into CHO cells cultured in Ham's F12 medium supplemented with 10% fetal bovine serum at 37°C, in 5% $CO_2$, using Lipofectamine LTX reagent (Life Technologies) according to the manufacturer's instructions.

### *Immunofluorescent laser-scanning confocal microscopy*

Cells grown on coverslips coated with 100 μg/ml fibrinogen were fixed with 4% paraformaldehyde, followed by permeabilization with phosphate-buffered saline containing 0·1% Triton X100. After blocking, the cells were stained with primary antibodies at appropriate dilutions, followed by staining with Alexa488- or Cy3-conjugated secondary antibodies together with Hoechst 33342. High-resolution immunofluorescent images were taken under a laser-scanning confocal microscopy (LSM5 Pascal, Carl Zeiss, Oberkochen, Germany) using a x63 objective.

### *Flow cytometry*

The expression and activation of integrin αIIb and β3 on the platelet surface was indirectly estimated by flow cytometry with the antibodies described above. Mean fluorescence intensity (MFI) of values in an affected individual were divided by those in an unrelated normal control and recorded as relative MFI value (%). For the quantitative determination of αIIbβ3 molecules on the platelet surface, QIFIKIT (Dako, Glostrup, Denmark) was used according to the manufacturer's instructions. MFI of the calibration beads containing five populations (antibody-binding capacity: 2600, 9900, 46 000, 221 000 and 741 000) were 16·12, 63·83, 262·84, 1483·2 and 3772·1, respectively, whereas that of the negative control sample was 1·62. Therefore, αIIbβ3 molecules (copies/platelet) was calculated as $10^{(1·022 \times \log(\mathrm{MFI}) + 2·1679)} - 241$. Activation of platelets and CHO cells was estimated by methods previously described (Shattil *et al*, 1987; Hughes *et al*, 1996). Activation index was defined as $(F-F_0) / (F'-F_0)$, where F is the MFI of PAC-1-stained CHO cells transfected with αIIbβ3-L718P or αIIbβ3-D723H, and $F_0$ and F' are those transfected with αIIbβ3-WT and αIIbβ3-T562N, respectively. The samples were analyzed on a FACS Calibur (Becton Dickinson, Franklin Lakes, NJ, USA), equipped with an argon laser operating at 488 nm.



© 2012 Blackwell Publishing Ltd

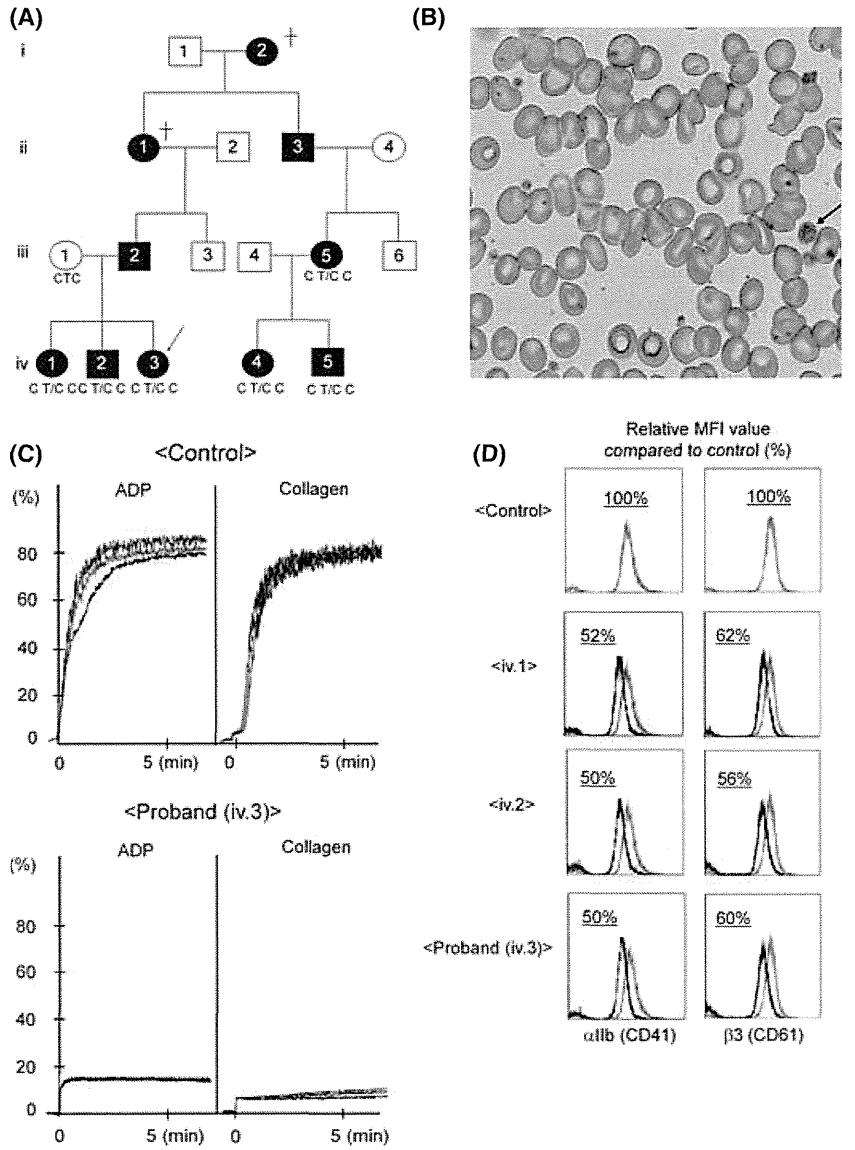


Fig 1. Platelet morphology and aggregation tracings. (A) The pedigree shows affected (filled) and unaffected (open) females (circles) and males (squares). The patient is indicated by an arrow. (B) Platelet morphology as determined by optical microscopy. Peripheral blood specimen obtained from the patient stained with May-Giemsa. The arrow indicates a macrothrombocyte. Original magnification × 600. (C) Representative platelet aggregation tracings in response to ADP and collagen stimuli in platelet-rich plasma from the patient and an unrelated normal control. (D) Flow cytometry of surface integrin αIIb (CD41) and β3 (CD61) expression. Samples were obtained from three affected individuals of the pedigree and an unrelated normal control. Data were calculated as relative MFI value (%), where MFIs of affected individuals were divided by MFI of a control sample.

*Exome sequencing*

Genomic DNA was obtained from four affected individuals in the pedigree and whole exome sequencing was performed. Briefly, 3 μg genomic DNA was fragmented by Covaris S2 (Covaris, Woburn, MA, USA) and ligated to adaptors, followed by hybridization to biotinylated RNA baits according to the manufacturer's instruction (Agilent Technologies, Santa Clara, CA, USA). The generated sequence tags were sequenced by the 76 bp paired-end protocol of Illumina GAIIx (Illumina, San Diego, CA, USA) and mapped onto the human genomic sequence (hg18, UCSC Genome Browser) using the sequence alignment program Eland (Illumina). Unmapped or redundantly mapped sequences were removed from the data set, and only uniquely mapped sequences were used for further analyses. Positions relative to RefSeq genes were calculated based on the respective genomic coordinates. Genomic coordinates of exons and the protein-coding regions of the RefSeq transcripts are as described in hg18. To verify the presence of *ITGB3* gene alteration, amplification and direct sequencing of a part of exon 14 was performed with the following primers; 5′-CATAGCCAGTTCAAGTGACTCCTG-3′ for forward primer and 5′-ACGATGGTACTGGCTGAACATGAC-3′ for reverse primer.

## Results

*Pedigree of a family with autosomal dominant thrombocytopenia with anisocytosis*

In the original patient, marked platelet anisocytosis was observed in peripheral blood samples (Fig 1B). Platelet aggregation induced by ADP (1–4 μmol/l) and collagen (0·5–2 μg/ml) was markedly reduced (Fig. 1C and Table I), but agglutination induced by ristocetin (1·25 mg/ml) was within

© 2012 Blackwell Publishing Ltd

the normal range (data not shown). Three affected individuals (iii.5, iv.1, and iv.2) showed abnormalities in platelet function similar to those of the original patient. In these affected individuals, the αIIb and β3 expression levels, which were indirectly estimated as relative MFI value (%), were 43–75% of a healthy control (Fig 1D and Table I). The number of αIIbβ3 molecules on the platelet surface in patients, as evaluated by flow cytometry using QIFIKIT, was 35 000–38 400 copies/platelet (MFI: 212·1 –232·4), whereas in an unaffected individual of the pedigree (iii.1) and an unrelated control, there were 65 200 and 62 100 copies/platelet (MFI: 389·2 and 371·3), respectively (Table I). The tendency to bleed was mild to moderate, as exemplified by the following episodes: when family member iv.1 received a bruise to the face, treatment with recombinant Factor VIIa was required because of persistent epistaxis; also, family member iii.5 had had to give birth by Caesarean section because of low platelet count. The family pedigree (Fig 1A), which shows no evidence of consanguineous marriage, strongly suggests the inheritance of thrombocytopenia as an autosomal dominant trait. The laboratory findings are shown in Table I.

### *Identification of the integrin β3 L718P mutation by whole exome analysis*

To isolate a candidate gene alteration responsible for the thrombocytopenia, whole exome sequencing analysis was performed using genomic DNA obtained from the patient (iv.3), her sister and brother (iv.1 and iv.2) and a cousin (iv.4). A total of 794 non-synonymous gene alterations among 1551 SNPs that are not registered in dbSNP 129/130 were detected in the patient. To isolate the responsible gene, we selected non-synonymous gene alterations shared by the four affected individuals as strong candidates. Among the 90 alterations commonly found in the affected individuals of the pedigree (individual numbers of SNPs/mutations are shown in Table II), we focused on the heterozygous non-synonymous T2231C alteration in exon 14 of the *ITGB3* gene, which results in the substitution of leucine at 718 for proline (L718P) in the integrin β3 protein. We selected this because it was recently reported as a candidate mutation responsible for thrombocytopenia (Jayo *et al*, 2010). The presence of the mutation in six affected individuals of the pedigree (iv.1, iv.2, iv.3, iv.4, iii.5 and iv.5) and its absence in an unaffected individual (iii.1) and an unrelated control was confirmed by a direct-sequencing (Fig 2). As far as we could determine, no other non-synonymous gene alterations previously reported to cause thrombocytopenia or defective platelet function were present in the affected individuals of the pedigree. In addition, the L718 residue in integrin β3 is well-conserved between species and amino acid substitution in this position is predicted by bioinformatic tools, including Polyphen and SIFT, to cause a significant change in protein structure and function (data not shown). These observations strongly suggest that the L718P mutation in integrin β3 is the responsible gene alteration that causes familial thrombocytopenia.

### *Constitutive but partial activation of the αIIbβ3 complex by β3-L718P*

To elucidate the effects of the integrin β3-L718P mutation on the activation status of αIIbβ3 complexes in resting or ADP-activated platelets, fresh platelets were analysed by flow cytometry using PAC-1, a ligand-mimicking antibody that specifically recognizes the activated form of the αIIbβ3 complex (Shattil *et al*, 1987).

Resting control platelets from healthy individuals bound PAC-1 with a similar affinity to those treated with RGDS, a peptide which competitively inhibits the binding of ligands for

**Table I.** Laboratory data of seven individuals of the pedigree.

| | | | | | | Relative MFI value compared to control (%) | | αIIbβ3 molecules | | Platelet aggregation (%) | |
|---|---|---|---|---|---|---|---|---|---|---|---|
| Patient | Sex | Age (years) | Platelet count ($\times 10^9$/l) | MPV (fl) | PDW (%) | αIIb | β3 | MFI | copies/platelet | ADP (4 μM) | collagen (2·0 μg/ml) |
| iii.1 | F | 37 | 210 | 10·2 | 12·1 | 110 | 111 | 389·2 | 65 200 | NA | NA |
| iii.5 | F | 34 | 38–67 | 8·5–11·3 | 10·0–19·0 | 43 | 75 | NA | NA | 15 | 12 |
| iv.1 | F | 11 | 30–43 | 7·8–11·2 | 9·7–16·3 | 52 | 62 | 232·4 | 38 400 | 16 | 8 |
| iv.2 | M | 8 | 49–64 | 10·3–11·1 | 10·1–14·7 | 50 | 56 | 216·4 | 35 700 | 23 | 16 |
| iv.3 | F | 6 | 49–72 | 9·8–10·9 | 11·1–13·3 | 50 | 60 | 212·1 | 35 000 | 12 | 8 |
| iv.4 | F | 4 | 32–59 | 9·9–10·8 | 12·3–15·6 | NA | NA | NA | NA | NA | NA |
| iv.5 | M | 2 | 28–50 | 8·9–9·0 | 18·0–18·4 | 49 | 51 | NA | NA | NA | NA |

MPV, mean platelet volume (normal range: 9·4–12·3 fl); PDW, platelet distribution width (normal range: 9·5–14·8 %); NA, not available.
αIIbβ3 molecules (copies/platelet) were calculated as $10^{(1.022 \times \log(\mathrm{MFI}) + 2.1679)} - 241$ (see *Materials and methods*).



© 2012 Blackwell Publishing Ltd

Table II. Number of SNPs/mutations detected by whole exome sequencing.

| Case | iv.1 | iv.2 | iv.3 | iv.4 |
|---|---|---|---|---|
| SNP | 21 531 | 21 697 | 20 413 | 20 113 |
| Not in dbSNP 129 and 130 | 1 674 | 1 722 | 1 473 | 1 551 |
| Non-synonymous alternations | | | | |
| Homozygous | 62 | 58 | 65 | 42 |
| Heterozygous | 800 | 815 | 667 | 752 |
| Non-synonymous (common) | 90 | | | |

αIIbβ3 complex such as fibrinogen and PAC-1 (Fig 3A, compare black and blue lines), indicating that wild-type αIIbβ3 in resting platelets is not activated. In contrast, platelets obtained from the affected individuals (iii.5, iv.1, iv.2 and iv.3) showed a slight increase of PAC-1 binding compared to those treated with RGDS (Fig 3A). Indeed, resting platelets from affected individuals showed a slight but significant increase of PAC-1 binding relative to healthy individuals (Fig 3A, top panel). In addition, flow cytometric analysis using FITC-conjugated fibrinogen also showed a significant increase of fibrinogen binding potential in resting platelets from affected individuals compared with healthy controls (bottom panel). Because MPV (shown in Table I) did not exceed the normal range (9·4–12·3 fl) and surface expression levels of αIIbβ3 were lower in patients than controls (Fig 1D), it is proposed that these observations indicate spontaneous activation of αIIbβ3-L718P in resting platelets.

ADP-activated platelets from healthy volunteers, on the other hand, bound to PAC-1 with a very high affinity (Fig 3B, red lines and 3B, top panel), as expected. In contrast, only a small increase of affinity to PAC-1 was observed in ADP-treated platelets carrying the β3-L718P mutation, resulting in a marginal increase of binding potential (bottom panel). These findings suggest that αIIbβ3-L718P is partially activated in the absence of inside-out signals such as ADP, but nevertheless cannot be fully activated in the presence of such signals.

To confirm the contribution of the integrin β3-L718P mutation to spontaneous activation of αIIbβ3, CHO cells were transiently transfected with expression vectors encoding integrin β3-WT, -L718P, -D723H or -T562N together with a vector encoding αIIb-WT. Flow cytometric analysis (Fig 3C) revealed that αIIbβ3-L718P expressed in CHO cells bound to PAC-1 to the same degree as αIIbβ3-D723H, a mutant previously reported to partially activate αIIbβ3, and to a lesser extent than a fully active αIIbβ3-T562N mutant (Kashiwagi *et al*, 1999). We calculated the activation indices (see *Materials and methods*) (Hughes *et al*, 1996; Schaffner-Reckinger *et al*, 2009) of αIIbβ3-L718P and -D723H as 0·23 ± 0·07 and 0·16 ± 0·02, respectively, taking αIIbβ3-T562N as fully active (=1·0) and αIIbβ3-WT as inactive (=0) (Fig 3D). Because CHO cells were not stimulated by ADP in this experiment, each index represents αIIbβ3 activation status at rest.

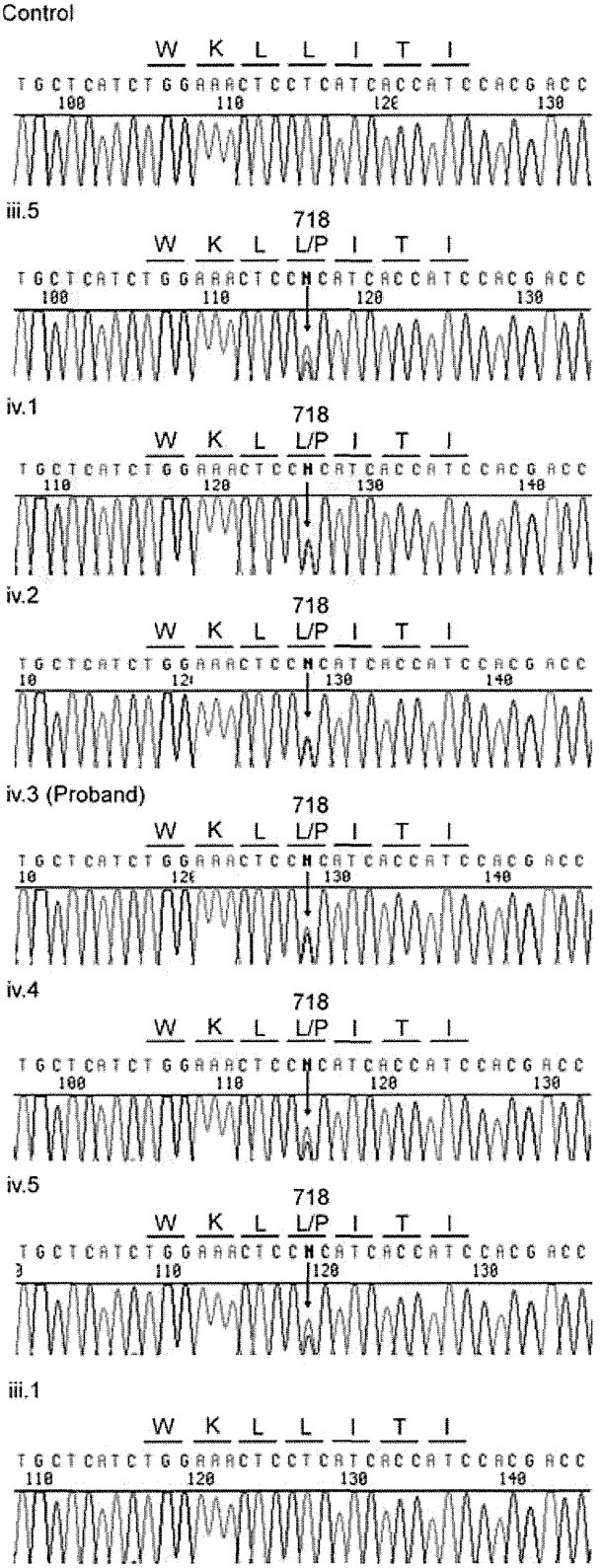


Fig 2. Direct sequencing analysis around T2231 in exon 14 of the *ITGB3* gene. Genomic DNA extracted from the affected and unaffected individuals of the pedigree were amplified by polymerase chain reaction and sequenced. Arrows indicate the position of the T2231 mutation in the *ITGB3* gene.

© 2012 Blackwell Publishing Ltd

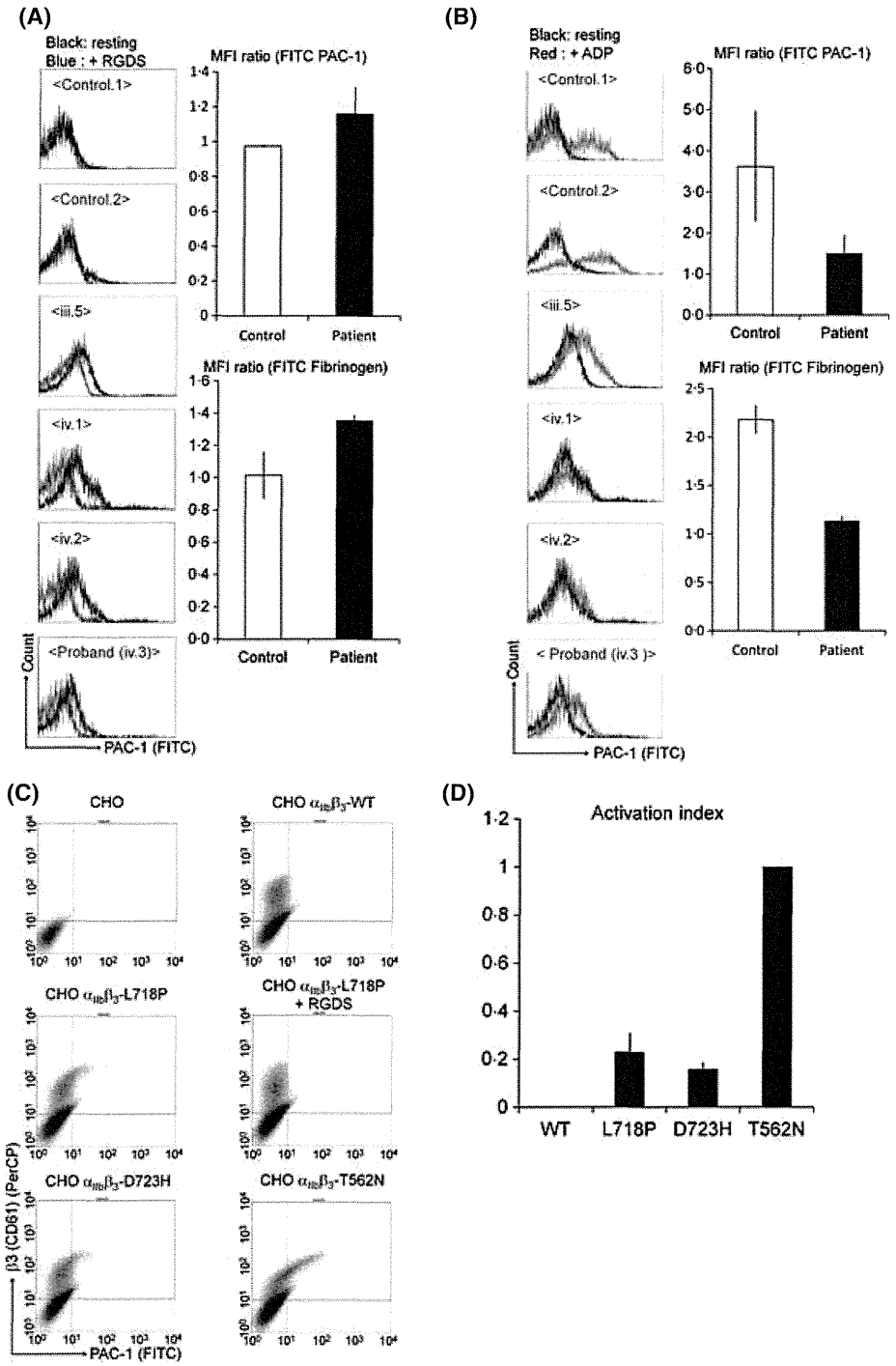


Fig 3. Functional analysis of integrin β3-L718P mutation. (A) Spontaneous binding of PAC-1 antibody to platelets obtained from affected individuals of the pedigree. Non-activated platelets (within 10 min after blood collection), incubated with or without 1 mM RGDS, were stained with FITC-conjugated PAC-1 antibody. After fixation, binding of PAC-1 to platelets was analysed by flow cytometry. Activation status of αIIbβ3 complex on resting platelets bound to FITC-PAC-1 (top) and FITC-fibrinogen (bottom). Mean fluorescence intensity (MFI) ratio was estimated by dividing the MFI of resting platelets by that of resting platelets incubated with RGDS. (B) Reduced activation of αIIbβ3 from affected individuals. The resting and ADP-stimulated platelets, stained with FITC-conjugated PAC-1 antibody were analysed by flow cytometry. Activation status of αIIbβ3 on stimulated platelets bound to FITC-PAC-1 (top) and FITC-fibrinogen (bottom). Values were estimated by dividing the MFI of platelets stimulated with ADP by those of resting platelets. (C) Partial activation of αIIbβ3-L718P and -D723H on CHO cells. CHO cells transfected with αIIbβ3 expression vectors (β3-WT, -L718P, -D723H and -T562N) were seeded on 100 μg/ml fibrinogen-coated coverslips in 6-well dishes. The cells, treated with or without RGDS, were stained with FITC-conjugated PAC-1 antibody and PerCP-conjugated anti-CD61 antibody and analysed by flow cytometry. (D) Activation index of αIIbβ3 mutants. Activation status of CHO cells expressing αIIbβ3-L718P and -D723H was compared with that of αIIbβ3-T562N as described in the "*Materials and methods*".



© 2012 Blackwell Publishing Ltd

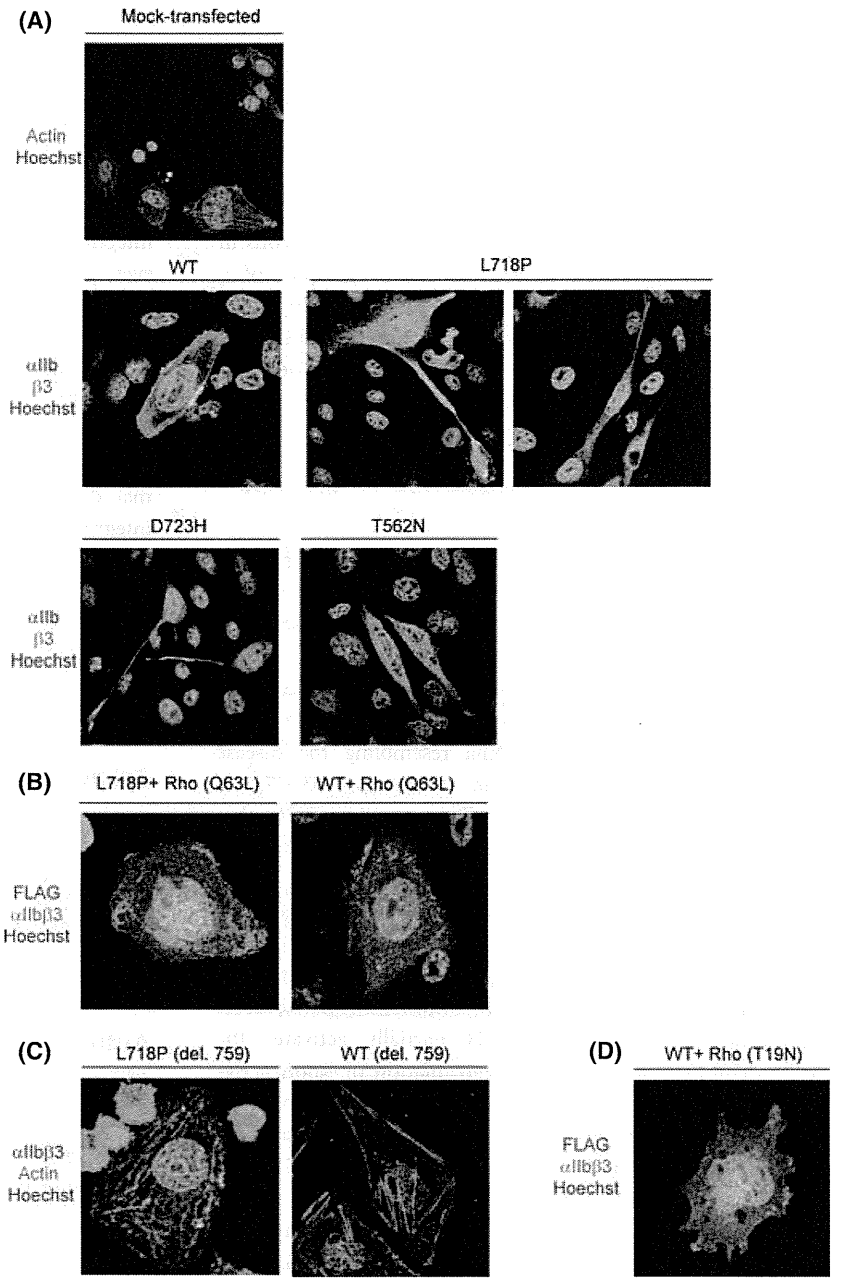


Fig 4. Overexpression of RhoA mutants or integrin β3-L718P (del. 759) modulates the formation of proplatelet-like cell protrusions in CHO cells. (A) Changes in CHO cell morphology by αIIbβ3 mutants. CHO cells transfected with αIIbβ3-L718P, -T562N and -D723H were seeded on fibrinogen-coated coverslips. After an 8-h incubation, the cells were fixed and stained with anti-CD41 and -CD61 antibodies followed by staining with Cy3- and Alexa 488-conjugated secondary antibodies. Mock-transfected cells were stained with Alexa 488-conjugated phalloidin and Hoechst 33342. (B) Inhibition of proplatelet-like protrusion formation by constitutively-active RhoA. An expression vector that encodes FLAG-tagged RhoA (Q63L) was transfected together with αIIbβ3-L718P or -WT expressing vectors into CHO cells. The cells grown on fibrinogen-coated coverslips were fixed and stained with anti-CD41 and anti-DDDDK-tag antibodies followed by staining with Alexa 488- and Cy3-conjugated secondary antibodies. (C) C-terminal deletion of β3-L718P inhibits the formation of proplatelet-like protrusions. C-terminal deleted integrin β3-L718P or -WT (del. 759) was expressed together with αIIb in CHO cells. The cells were fixed and stained with anti-CD41 antibody followed by staining with Cy3-conjugated secondary antibody and Alexa-488-labeled phalloidin. (D) A dominant-negative (T19N) form of RhoA was overexpressed in CHO cells. Images were taken as in (B).

### *Involvement of RhoA signalling in proplatelet-like protrusion formation*

As previously reported by others (Ghevaert *et al*, 2008; Jayo *et al*, 2010), CHO cells expressing αIIbβ3-L718P, as well as αIIbβ D723H, formed long proplatelet-like protrusions on fibrinogen-coated dishes that were not observed in cells expressing wild-type αIIbβ3 (Fig 4A). In contrast, although cells expressing αIIbβ3-T562N, which yields a fully activated conformation (Kashiwagi *et al*, 1999), changed from their original round shape surrounded by a broad protrusion (Fig 4A, mock-transfected) to rhomboid-like cell morphology, proplatelet-like protrusions were rarely seen (Fig 4A). This suggests that mutants partially activating the integrin complex induce long proplatelet-like protrusions.

Recently, it was reported that the formation of proplatelet-like protrusions in CHO cells is mediated by the downregulation of RhoA activity (Chang *et al*, 2007; Schaffner-Reckinger *et al*, 2009), which is initiated by the binding of c-Src to the C-terminal tail (amino acid 760–762, Arg-Gln-Thr; RGT) of integrin β3 (Flevaris *et al*, 2007). We found that the formation of long cell protrusions was inhibited when a constitutively-active form of RhoA (Q63L) was introduced into αIIbβ3-L718P-expressing cells (Fig 4B). In addition, CHO cells expressing αIIbβ3-L718P (del. 759) mutant, which lacks the C-terminal c-Src binding site of in-

© 2012 Blackwell Publishing Ltd

tegrin β3 (RGT), did not form any proplatelet-like protrusions (Fig 4C). Given that enforced activation of RhoA caused by introducing RhoA (Q63L), as well as de-repression of RhoA through C-terminal deletion of β3 in cells expressing αIIbβ3-WT, did not induce morphological changes in CHO cells (Figs 4B, C), it is proposed that constitutive inhibition but not activation through the c-terminal of β3 is responsible for the formation of abnormal cell protrusions in L718 mutants. However, as the enforced expression of a dominant negative form of RhoA (T19N) in αIIbβ3-WT expressing cells did not result in typical proplatelet-like protrusions (Fig 4D), this suggests that downregulation of RhoA was required but not sufficient for the formation of proplatelet-like protrusions induced by integrin β3-L718P.

## Discussion

We report a pedigree with individuals suffering from a lifelong haemorrhagic syndrome, all of whom were carrying the integrin β3-L718P mutation. This had previously been reported only in a sporadic patient (Jayo *et al*, 2010). Next-generation sequencing, together with the clinical data of the patients, established that this integrin β3-L718P mutation causes thrombocytopenia resembling the disease caused by a different integrin mutation, β3-D723H, although the size of the platelets seems to differ somewhat between these mutations (Ghevaert *et al*, 2008; Schaffner-Reckinger *et al*, 2009).

Considering the dominant inheritance pattern of the haemorrhagic tendency caused by integrin β3-L718P as well as β3-D723H, these would be gain of function mutations, unlike those causing Glanzmann thrombasthenia. Indeed, expression of integrin β3-D723H partially activates the αIIbβ3 complex, resulting in downregulation of RhoA activity and induction of microtubule-dependent proplatelet-like cell protrusions considered relevant for production of macrothrombocytes (Ghevaert *et al*, 2008; Schaffner-Reckinger *et al*, 2009). Integrin β3-L718P appears to act in a similar fashion (Fig 4A and B). Interestingly, we demonstrate that the three C-terminal amino acid residues (RGT) of integrin β3 are required for L718P to form proplatelet-like cell protrusions (Fig 4C). RGT provides a binding site for c-Src tyrosine kinase, which was shown to inactivate RhoA (Flevaris *et al*, 2007), further supporting the hypothesis that integrin β3-L718P plays a role in causing megakaryocytes to produce abnormal platelets through the inhibition of RhoA.

In platelets derived from megakaryocytes that carry the integrin β3-L718P mutation, full activation of αIIbβ3 complex in response to inside-out stimuli is inhibited, as shown by reduced binding of PAC-1 and fibrinogen on stimulation with ADP (Fig 3B). A simple scenario is that, in platelets, integrin β3-L718P acts as a loss of function mutation. However, given that the carriers of Glanzmann's thrombasthenia who have both normal and mutant allele and express reduced amounts of the αIIbβ3 complex, in general show normal platelet aggregation, it is possible that the integrin β3-L718P mutation gains a function that ultimately results in the reduction of inside-out signals.

In summary, identification of a pedigree showing autosomal dominant inheritance leads to a model whereby the integrin β3-L718P mutation contributes to thrombocytopenia accompanied by anisocytosis most likely through gain-of-function mechanisms. Further investigations are necessary to fully elucidate these mechanisms by which this mutation exerts its abnormal effect on thrombocytosis and platelet aggregation.

## Acknowledgements

We thank Prof. M. Matsumoto and Ms. M. Sasatani for providing clinical data; Ms. M. Nakamura, Ms. E. Kanai and Ms. R. Tai for excellent technical assistance. This work was partly supported by Grants-in-Aid for Scientific Research from the Ministry of Health, Labour and Welfare of Japan.

## Author contributions

H.M., T.I. and M.K. designed the work. Y.K., H.M., A.K., S.O. and M.T. performed experiments and analysed data. S.K. contributed essential materials and interpreted data. M.M and K.N. contributed clinical materials and data. H.M, Y.K. and T.I. wrote the manuscript.

## Conflict of interest

The authors declare no competing financial interests.

## References

Chang, Y., Auradé, F., Larbret, F., Zhang, Y., Couedic, J.P.L., Momeux, L., Larghero, J., Bertoglio, J., Louache, F., Cramer, E., Vainchenker, W. & Debili, N. (2007) Proplatelet formation is regulated by the Rho/ROCK pathway. *Blood*, **109**, 4229–4236.

Flevaris, P., Stojanovic, A., Gong, H., Chishti, A., Welch, E. & Du, X. (2007) A molecular switch that controls cell spreading and retraction. *Journal of Cell Biology*, **179**, 553–565.

George, J.N., Caen, J.P. & Nurden, A.T. (1990) Glanzmann's thrombasthenia: the spectrum of clinical disease. *Blood*, **75**, 1383–1395.

Ghevaert, C., Salsmann, A., Watkins, N.A., Schaffner-Reckinger, E., Rankin, A., Garner, S.F., Stephans, J., Smith, G.A., Debili, N., Vainchenker, W.de, Groot, P.G., Huntington, J.A., Laffan, M., Kieffer, N. & Ouwehand, W.H. (2008) A non-synonymous SNP in the ITGB3 gene disrupts the conserved membrane-proximal cytoplasmic salt bridge in the αIIbβ3 integrin and cosegregates dominantly with abnormal proplatelet formation and macrothrombocytopenia. *Blood*, **111**, 3407–3414.

Hughes, P.E., Diaz-Gonzalez, F., Leong, L., Wu, C., McDonald, J.A., Shattil, S.J. & Ginsberg, M. H. (1996) Breaking the integrin hinge. A defined structural constraint regulates integrin signaling. *Journal of Biological Chemistry*, **271**, 6571–6574.

Jayo, A., Conde, I., Lastres, P., Martinez, C., Rivera, J., Vicente, V. & Manchón, C.G. (2010) L718P mutation in the membrane-proximal



© 2012 Blackwell Publishing Ltd

cytoplasmic tail of β3 promotes abnormal αIIbβ3 clustering and lipid domain coalescence, and associates with a thrombasthenia-like phenotype. *Haematologica*, **95**, 1158–1166.

Kashiwagi, H., Tomiyama, Y., Tadokoro, S., Honda, S., Shiraga, M., Mizutani, H., Honda, M., Kurata, Y., Matsuzawa, Y. & Shattil, S.J. (1999) A mutation in the extracellular cysteine-rich repeat region of the β3 subunit activates integrins αIIbβ3 and αVβ3. *Blood*, **93**, 2559–2568.

Kunishima, S., Kashiwagi, H., Otsu, M., Takayama, N., Eto, K., Onodera, M., Miyajima, Y., Takamatsu, Y., Suzumiya, J., Matsubara, K., Tomiyama, Y. & Saito, H. (2011) Heterozygous ITGA2B R995W mutation inducing constitutive activation of the αIIbβ3 receptor affects proplatelet formation and causes congenital macrothrombocytopenia. *Blood*, **117**, 5479–5484.

Nurden, A.T. (2006) Glanzmann thrombasthenia. *Orphanet Journal of Rare Diseases*, **1**, 10.

Nurden, P. & Nurden, A.T. (2008) Congenital disorders associated with platelet dysfunctions. *Thrombosis and Haemostasis*, **99**, 253–263.

Nurden, A.T., Fiore, M., Nurden, P. & Pillois, X. (2011a) Glanznmann thrombasthenia: a review of ITGA2B and ITGB3 defects with emphasis on variants, phenotype variability, and mouse models. *Blood*, **118**, 5996–6005.

Nurden, A.T., Pillois, X., Fiore, M., Heilig, R. & Nurden, P. (2011b) Glanzmann thrombasthenia-like syndromes associated with macrothrombocytopenias and mutations in the gene encosing the αIIbβ3 integrin. *Seminars in Thrombosis and Hemostasis*, **37**, 698–706.

Schaffner-Reckinger, E., Salsmann, A., Debili, N., Bellis, J., Demey, J., Vainchenker, W., Ouwehand, W.H. & Kieffer, N. (2009) Overexpression of the partially activated αIIbβ3D723H integrin salt bridge mutant downregulates RhoA activity and induces microtubule-dependent proplatelet-like extensions in Chinese hamster ovary cells. *Journal of Thrombosis and Haemostasis*, **7**, 1207–1217.

Shattil, S.J., Cunningham, M. & Hoxie, J.A. (1987) Detection of activated platelets in whole blood using activation-dependent monoclonal antibodies and flow cytometry. *Blood*, **70**, 307–315.

© 2012 Blackwell Publishing Ltd